Scaling of the Hall resistivity in the solid and liquid vortex phases in twinned single-crystal $YBa_2Cu_3O_{7-\delta}$

G. D'Anna, V. Berseth, and L. Forró
Institut de Génie Atomique, Ecole Polytechnique Fédérale de Lausanne, CH-1015 Lausanne, Switzerland

A. Erb and E. Walker
Département de Physique de la Matière Condensée, Université de Genève, CH-1211 Genève, Switzerland

(Received 15 March 1999; revised manuscript received 1 October 1999)

Longitudinal and Hall voltages are measured in a clean twinned $YBa_2Cu_3O_{7-\delta}$ single crystal in the liquid and solid vortex phases. For magnetic fields tilted away from the *c* axis more than about 2°, a scaling law $|\rho_{xy}| = A\rho_{xx}^{\beta}$ with $\beta \approx 1.4$ is observed, which is unaffected by the vortex-lattice melting transition. The vortex-solid Hall conductivity is nonlinear and diverges to negative values at low temperature. When the magnetic field is aligned to the *c* axis, the twin-boundary correlated disorder modifies the scaling law, and $\beta \approx 2$. The scaling law is unaffected by the Bose-glass transition. We discuss the scaling behavior in terms of a dimension-dependent percolation theory. The twin-boundary guided vortex motion is also investigated.

I. INTRODUCTION

A current flowing in a conductor exposed to a magnetic field gives rise to a Hall voltage. The Hall effect has been a powerful probe of the mechanisms of charge transport in metals and semiconductors. Similarly, a Hall voltage is observed in superconductors in high magnetic fields and carrying large electric currents. The Hall effect in this system is an intriguing phenomenon that has triggered a very large experimental and theoretical literature. Remarkable experimental facts include the ''Hall anomaly,'' i.e., the Hall-effect sign reversal in the superconducting vortex state with respect to the normal state, as observed in various high- and low-temperature type-II superconductors,[1] and the Hall resistivity ''scaling law'' $\rho_{xy} \propto \rho_{xx}^{\beta}$ with $1 \leqslant \beta \leqslant 2$ (ρ_{xy} is the Hall resistivity, ρ_{xx} is the longitudinal resistivity).[2]

Many theoretical explanations have been proposed, most of them addressing the Hall anomaly, which is believed to be a fundamental problem of vortex dynamics. These theories are developed either in terms of microscopic electronic processes,[3–7] or including pinning,[8] vortex-vortex interactions,[9,10] time-dependent Ginzburg-Landau theories,[11] phenomenological models,[12–14] or other ideas.[15] The most frequently adopted approach is microscopic: it ascribes the Hall effect in the vortex state to hydrodynamic and vortex-core forces, which determine the single vortex trajectory (e.g., in Ref. 4). In the scenario the Hall anomaly results from microscopic details of the Fermi surface. However, a consensus is not achieved on fundamental points like the transverse force on a vortex moving in a superfluid,[16,17] or on experimental problems like the doping dependence.[18]

Some of these theories also predict the scaling law, in particular by including the pinning,[8] or considering vortex-lattice defects.[9] However, only two theories are specifically developed to explain the scaling law. Dorsey *et al.*[13] have proposed a scaling theory near the vortex-glass transition with an universal, sample independent power $\beta < 2$ for the three-dimensional regime. But the scaling is also seen when the vortex phase transition is not a vortex-glass transition. Vinokur *et al.*[12] proposed that the scaling law with strictly $\beta \equiv 2$ is a general feature of any vortex state with disorder-dominated dynamics, without the need to invoke the vortex-glass scaling. In this model the Hall conductivity is independent of disorder and is directly linked to the microscopic processes determining the single vortex equation of motion. This is in conflict with the spread of the observed β, and with the change of the Hall conductivity at the vortex-lattice melting transition.[19,20]

We report here measurements intended to study in particular the scaling law of the Hall resistivity in various vortex phases (e.g., Bragg-glass, Bose-glass, vortex-liquid) and across the different vortex phase transitions. We perform experiments in a twinned $YBa_2Cu_3O_{7-\delta}$ crystal, and by finely orienting the magnetic field parallel or at an angle to the twin boundaries we can tune between the different vortex phases. We will show that the scaling law observed in the vortex-liquid remains unchanged in the vortex solid phases (Bragg-glass or Bose-glass). When the magnetic field is parallel to the twin boundaries, we obtain a critical exponent $\beta \approx 2$, corresponding to a constant Hall conductivity σ_{xy} below and slightly above the Bose-glass transition. This is the first time that an exponent of $\beta \approx 2$ is shown to correspond to a constant Hall conductivity. When the field is tilted away from the twin boundaries, we obtain $\beta \approx 1.4$. In this case the Hall conductivity is current dependent in the Bragg-glass and is influenced by the melting transition, demonstrating that the Hall conductivity *is* pinning dependent. Finally we tentatively propose a general model for the Hall resistivity scaling law, describing the progressive transition to a frozen (pinned) vortex assembly in terms of a percolation process. In the picture, random distributed domains of frozen vortices provide vanishing electric resistivity, while the remaining domains are dissipative. The theoretical exponent β is then dependent on the dimensionality of the vortex system only, in particular $\beta = 2$ in two-dimensions, as for vortices aligned to unidirectional strong correlated disorder (twins), and

$\beta=1.44$ for three-dimensions, as for pointlike disorder or splayed correlated defects.

Because of the presence of twin boundaries, guided vortex motion occurs in our sample, resulting in a symmetric part (with respect to the magnetic field) of the transverse resistivity, in addition of the antisymmetric ''true'' Hall effect. As this work will show, the guided vortex motion is not relevant to the conclusions we will obtain for the Hall effect. However, in order to dissipate doubts, we will show also the experiments on the guided vortex motion effect, although they could be omitted.

II. RESULTS

A. Sample and contacts

The transport experiments shown below are performed in a very clean twinned $YBa_2Cu_3O_{7-\delta}$ (YBCO) single crystal with a sharp resistive transition at about $T_c=93.5$ K. The microtwinned crystal has dimensions 0.9×0.4 mm^2 in the *a-b* plane, and thickness 24 μm in the *c* direction. The major twin family is at 135° from the long edge of the sample. Some untwinned domains and some twins at 90° from the dominant family are also present. A nine-gold contacts pattern has been deposited on the surface of the sample. Two kinds of experiments have been conducted.

(1) Using the contact configuration shown in Fig. 1(a), we are able to measure the usual Hall effect. In particular the longitudinal resistivity ρ_{xx} and Hall resistivity ρ_{xy} are measured simultaneously by injecting an ac+dc current, I_x, along the longest dimension of the crystal, and by measuring the in-phase voltages parallel, V_x, and perpendicular, V_y, to the current at the ac frequency (30 Hz). Notice that when the dc current component is absent we measure the usual longitudinal and Hall resistivities, while in the presence of a dc component we really measure dV/dI, i.e., the differential longitudinal and Hall resistivities. The measurement of the differential resistivity provides the sensitivity necessary to probe the moving vortex solid phases (see also the discussion concerning Fig. 6). The experimental method is presented in detail in Refs. 19 and 21. The Hall conductivity is obtained by $\sigma_{xy}=\rho_{xy}/(\rho_{xx}^2+\rho_{xy}^2)$, and the Hall angle θ_H by $\tan\theta_H=\rho_{xy}/\rho_{xx}$.

(2) Using the contact configuration shown in Fig. 1(b), we are able to orient the applied ac+dc current in any direction in the sample plane, and to measure the electric field modulus and direction. This will permit us to observe the guided vortex motion. The application of an orientable ac+dc current is obtained by two in-phase sources with ac and dc components, as explained in detail elsewhere.[21] β_j in the inset of Fig. 1(b) is the angle of the applied current density and β_E is the angle of the electric field in the same *x-y* reference frame. Magneto-optical observations[21] have clearly shown that the dominant twin family is at 135° in the *x-y* reference frame of Fig. 1(b). This will also be confirmed by the results on guided vortex motion in Sec. II C.

B. Identification of the vortex phases and phase transitions

We begin by showing the characteristic features in transport measurements usually associated to the vortex phase transitions,[22] and discussing the angular dependence.[23] The

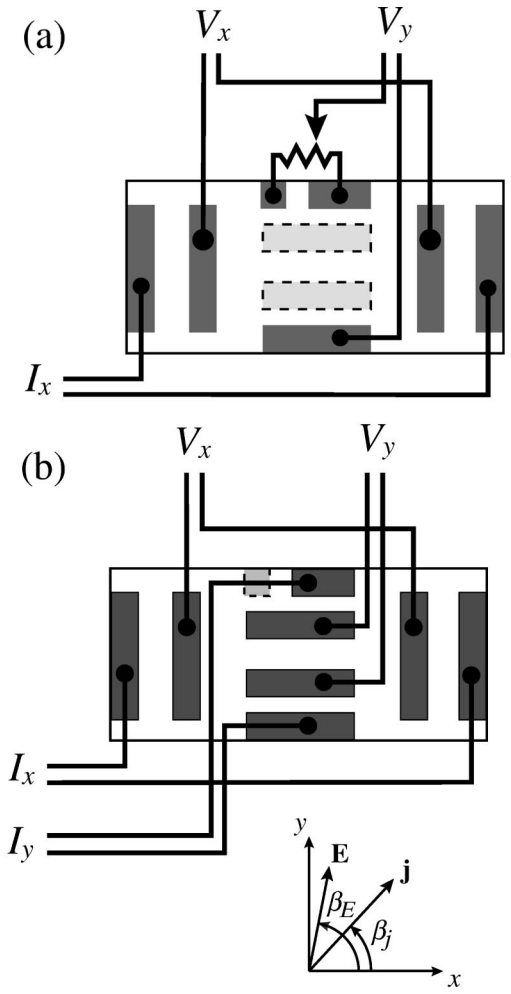

FIG. 1. Schematic contact connections for the Hall effect measurement. Of the nine contacts deposited on the crystal surface only seven are used in this configuration (the crystal is schematically shown as a rectangle. Proportions between sample dimensions and contact dimensions are close to reality). The Hall voltage is obtained from $[V_y(B)-V_y(-B)]/2$. (b) Schematic contact connection for the orientable electric current experiment for guided vortex motion. The ac+dc current can be oriented in any direction (noted β_j) in the plane of the sample, and the modulus $|E|$ and argument β_E of the resulting electric field measured. The *x-y* reference frame used is shown in the lower part of the figure. The dominant twin family is at 135° in this reference frame.

Bose-glass theory[24] predicts that for magnetic fields well aligned to the twin boundaries the vortex-solid phase is a smecticlike phase (Bose-glass) and the transition to the vortex-liquid is a Bose-glass transition. When the field is tilted away from the twin boundaries the vortex-solid phase is a Bragg-glass[25] and the transition to the vortex liquid is a vortex-lattice melting transition.

We found experimental evidence for this angular behavior. Figure 2 shows the longitudinal resistivity ρ_{xx} measured at 6 T for zero dc current and a small ac current of $j_{ac}=1$ A/cm^2, and for different angles α between the applied magnetic field and the *c* axis, as a function of the temperature. We use the contact configuration of Fig. 1(a). One can clearly see the effect of twin boundaries below T_{TB}. The twin-boundary pinning reduces the longitudinal resistivity, as expected for correlated disorder.[24]

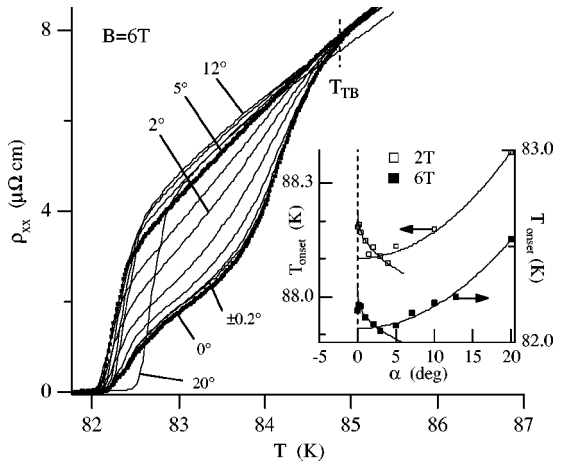

FIG. 2. The longitudinal resisitivity ρ_{xx} in a twinned $YBa_2Cu_3O_{7-\delta}$ single crystal at 6 T as a function of the temperature, measured at low-ac current density, $j_{ac}=1$ A/cm^2, for different angles between the field and the c axis ($-0.2°$,0°,0.2°,0.5°,1°,2°,3°,5°,7°,10°,12°,20°). Inset: the onset temperature T_{onset} as a function of the angle, at 2 T and 6 T. For about $\alpha>2°$ the onset temperature follows the usual anisotropic law of the vortex-lattice melting temperature. For small angles the onset temperature increases as expected from the Bose-glass theory (see text for details).

The inset of Fig. 2 shows the onset temperature T_{onset} of ρ_{xx} measured with a criterion of 0.1 $\mu\Omega$ cm, as a function of the angle. For decreasing, large angles $T_{onset}(=T_m)$ decreases according to a usual anisotropy law.[26] For small angles, the onset temperature $T_{onset}(=T_{BG})$ increases and reaches a maximum at $\alpha=0°$. This kind of behavior has been associated[23] to the change in the nature of the transition according to the Bose-glass theory. We have fitted the part of the data for small angles with the expression $T_{onset}(\alpha)=T_{onset,0}(1-\sin\alpha/x_c)^{1/3\nu}$, where $T_{onset,0}$, x_c, and ν are free parameters. The critical exponent ν is $\nu=1.23$ for $B=2$ T and $\nu=1.09$ for $B=6$ T, in agreement with the value of $\nu=1\mp0.2$ found by Grigera *et al.*[23] at $B=6$ T. The transition between the two regimes happens at an angle α^* of about 2°, consistently with the crossover angle $\alpha^*\approx2.1°$ of Ref. 23 for twinned YBCO crystals similar to the one we use. Notice that, since we have no thermodynamic data, we cannot affirm rigorously what the order of the vortex phase transitions we observe is. However, considering that the angular dependence is just the same as in Ref. 23, that our sample is much thinner than the crystals of same origin used for calorimetric measurements,[27] that it is very clean (it has very low normal state resistivity of 25 $\mu\Omega$ cm), we assume that the onset in resistivity in Fig. 1 can be associated to the vortex-lattice melting transition[22] for $\alpha>2°$, that we denote by T_m, and to the Bose-glass transition for $\alpha<2°$, that we denote by T_{BG}. Moreover, at the end of Sec. II D we provide experimental arguments supporting that the distinction of the two vortex-phases remains valid also when the two vortex-phases are driven by large electric currents.

C. Guided vortex motion

Having identified the crossover angle and the phase transitions, we now present the experiments concerning the influence of twin boundaries on vortex motion, using the contact configuration shown in Fig. 1(b), before addressing the Hall effect itself. The purpose of these experiments is to justify the statement that we can eliminate the influence of the vortex guided motion by extracting the antisymmetric part of the transverse resistivity upon magnetic field reversal. Using the contact configuration of Fig. 1(b) we can orient the ac+dc current in a given direction β_j in the sample plane, and measure the electric field modulus $|E|$ and direction β_E at the ac frequency. (The ac+dc electric current does not ''turn.'') The total current density used is $j=60$ A/cm^2 dc $+10$ A/cm^2 ac or $j=100$ A/cm^2 dc+25 A/cm^2 ac. Notice that by superimposing the ac current on top of a large dc current, the vortex-solid phases can be driven in motion under the effect of the large Lorentz force well below the vortex-lattice melting or Bose-glass transitions.

Figure 3(a) represents the evolution of the modulus $|E|$ (dashed lines) and argument β_E (plain lines) of the electric field as the magnetic field is reduced from $B=3$ T to 1 T, for a series of given current orientations β_j and at $\alpha=0°$. The total current density used is $j=60$ A/cm^2 dc+10 A/cm^2 ac. The orientation β_j of the current is indicated all around the polar plot. In other words, Fig. 3(a) represents $|E|(\beta_j)$ and $\beta_E(\beta_j)$ curves. The Bose-glass transition happens between the two curves separated by the shaded area. For a given current orientation β_j, the orientation of the electric field β_E is reported at the different fields. For example, follow the β_E line [the thicker line in Fig. 3(a)] when the current is oriented at $\beta_j=0°$. At high magnetic field, in the vortex liquid, the angle β_E is slightly shifted from zero by about $+5°$. This indicates the contact misalignment with the x and y axes. By decreasing magnetic fields the electric field progressively turns to $\beta_E\approx45°$ in the solid phase. This is a clear signature of the guided vortex motion along the dominant twin family at 135°. Notice that the effect is progressive and starts deep in the liquid phase, without sharp changes at the Bose-glass transition.

The guided vortex motion in the vortex solid phase (Bose-glass) is hardly visible in Fig. 3(a). In order to improve that, Fig. 3(b) is a polar plot of the electric field modulus $|E|$ as the current is rotated in the sample plane [that is, $|E|(\beta_j)$ curves] in the vortex solid phase at $B=2$ T and two different temperatures $T=88$ K and $T=87.5$ K (the Bose-glass transition is $T_{BG}\approx88.2$ K). The total current density used is $j=100$ A/cm^2 dc+25 A/cm^2 ac. Figure 3(b) nicely shows the influence of the dominant twin family and could be discussed in detail,[21] but for our purpose here it principally shows that at $\beta_j=0°$ [that is, the contact configuration of Fig. 1(a) used for usual Hall effect experiments below] *there is no absolute guided vortex motion* even in the Bragg-glass. Therefore, since the vortices have a trajectory not strictly parallel to the twin planes, the motion is influenced by the intrinsic Hall angle, and the (true) Hall effect can be extracted.

Exactly similar measurements have been performed with the magnetic field inclined at $\alpha=4°$, as shown in Fig. 4. In this case the vortex phase transition is the vortex-lattice melting, which happens between the two curves separated by the shaded area in Fig. 4(a). The guided vortex motion still occurs, as shown by the anisotropic shapes of Figs. 4(a) and 4(b), however the effect is less important and more gradual.

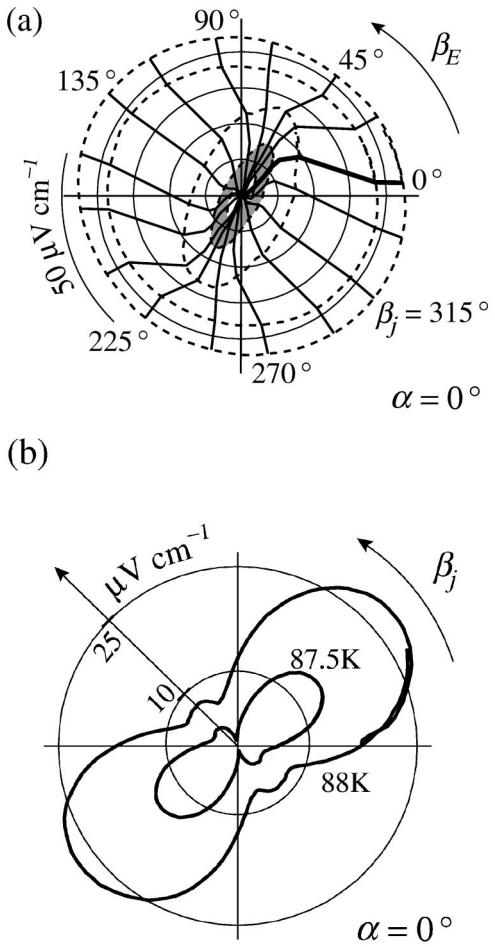

FIG. 3. Representation of the evolution of the modulus $|E|$ and argument β_E of the electric field, for a series of given current orientations β_j [that is, $|E|(\beta_j)$ and $\beta_E(\beta_j)$ curves], as the magnetic field is reduced from $B=3$ T to 1 T, obtained using the contact configuration of Fig. 1(b) with $\alpha=0°$, $T=89$ K and $j=60$ A/cm^2 dc$+10$ A/cm^2 ac. The orientations β_j are indicated around the plot. The continuous lines show the argument β_E of the electric field on a polar scale. The dashed lines show the modulus $|E|$ on a radial linear scale from 0 (center) to 50 μV cm^{-1}, for the magnetic fields $B=3$, 2.5, 2, 1.7, and 1.5 T (from outside towards the center). The Bose-glass transition occurs in the shaded area. (b) Polar plot of the electric field modulus $|E|$ as the current is rotated in the sample plane [that is, $|E|(\beta_j)$ curves] at $B=2$ T, $\alpha=0°$ and $j=100$ A/cm^2 dc$+25$ A/cm^2 ac for $T=88$ K and $T=87.5$ K. At these temperatures we are in the vortex-solid phase (Bose-glass).

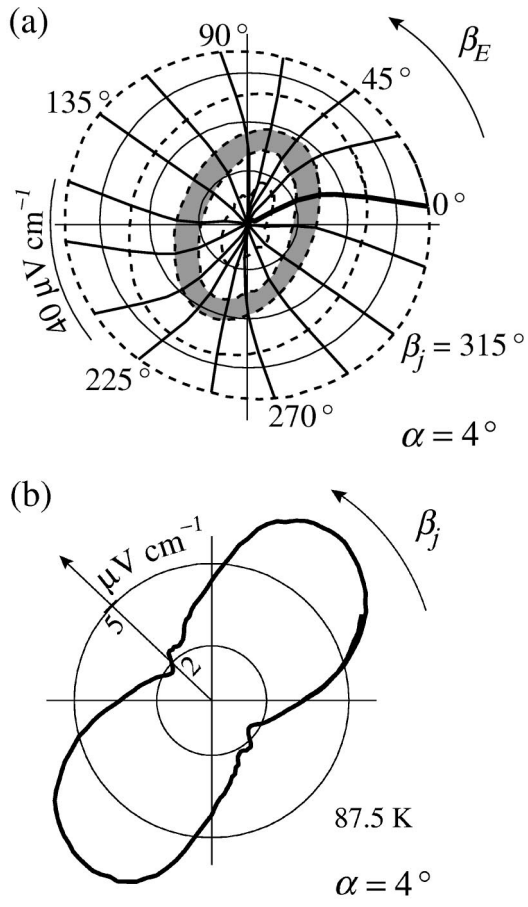

FIG. 4. Same as Fig. 3, but for $\alpha=3°$. (a) Representation of the evolution of the modulus $|E|$ and argument β_E of the electric field, for a series of given current orientations β_j, as the magnetic field is reduced from $B=2.5$ T to 1 T, obtained using the contact configuration of Fig. 1(b) with $\alpha=4°$, $T=89$ K and $j=60$ A/cm^2 dc $+10$ A/cm^2 ac. The orientations β_j are indicated around the plot. The continuous lines show the argument β_E of the electric field on a polar scale. The dashed lines show the modulus $|E|$ on a radial linear scale from 0 (center) to 40 μV cm^{-1}, for the magnetic fields $B=2.5$, 2, 1.7, 1.6, and 1.5 T (from outside towards the center). The vortex-lattice melting occurs in the shaded area. (b) Polar plot of the electric field modulus as the current is rotated in the sample plane at $B=2$ T, $\alpha=4°$ and $j=100$ A/cm^2 dc$+25$ A/cm^2 ac for $T=87.5$ K. At this temperature we are in the vortex-solid phase (Bragg-glass).

For example, the thicker line in Fig. 4(a), when the current is oriented at $\beta_j=0°$, shows that by decreasing the magnetic field the electric field progressively turns, but only to about 30°. Finally, the same conclusions obtained for $\alpha=0°$ concerning the influence of the guided vortex motion on the Hall measurements, are obtained for $\alpha=4°$, that is, Fig. 4(b) shows that in the vortex-solid at $\beta_j=0°$ there is no absolute guided motion.

D. Hall effect

The previous section has shown that we can eliminate the influence of the guided vortex motion on the Hall effect by extracting the antisymmetric part of the transverse resisitivity upon magnetic field reversal in the contact configuration of Fig. 1(a). They also have revealed no sharp change of the guided vortex motion at the vortex phase transition, eliminating the possibility that twin boundaries could explain the sharp change of the Hall conductivity at the vortex-lattice melting.[19] With all this in hand, we will now present the results of the Hall effect using the standard contact configuration shown in Fig. 1(a). The inset of Fig. 5 shows the Hall conductivity σ_{xy} as a function of the temperature at 2 T and at $\alpha=7°$ and $\alpha=0°$, measured with large dc and ac current densities ($j_{dc}=150$ A/cm^2, $j_{ac}=50$ A/cm^2) so that the Hall signal is detected deep inside the vortex-solid. In the inset the small difference in temperature between the vortex-lattice melting transition at T_m for $\alpha=7°$ and the Bose-glass transition at T_{BG} for $\alpha=0°$ is not visible. By reducing the temperature from the normal state the Hall conductivity σ_{xy}

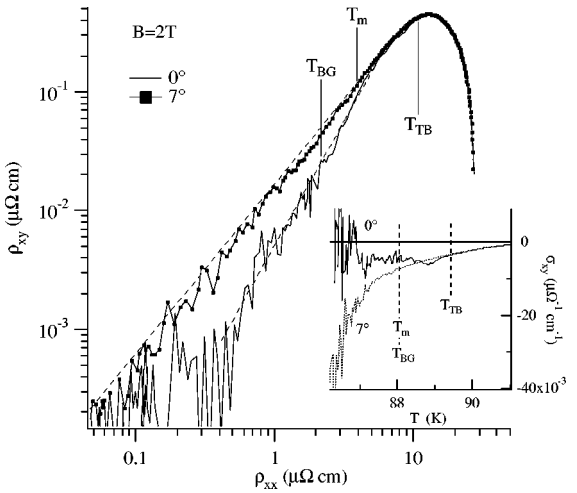

FIG. 5. Log-log plot of $|\rho_{xy}|$ vs ρ_{xx} at 2 T and $\alpha=7°$ and $\alpha=0°$. The linear fit according to a scaling law $|\rho_{xy}|=A\rho_{xx}^{\beta}$ gives $\beta\approx1.4$ for $\alpha=7°$, and $\beta\approx2.0$ for $\alpha=0°$, as indicated by the two straight dashed lines. The position of the vortex-lattice melting temperature, T_m, and of the Bose-glass temperature, T_{BG}, are indicated in the curves, as well as the temperature of twin-boundary pinning onset, T_{TB}. Notice that the scaling law is unaffected by crossing the transitions. Inset: the Hall conductivity, $\sigma_{xy}=\rho_{xy}/(\rho_{xx}^2+\rho_{xy}^2)$, as a function of the temperature at $\alpha=7°$ and $\alpha=0°$. The dashed vertical lines denote the transitions at T_m, T_{BG}, and T_{TB}. The current densities are $j_{dc}=150$ A/cm^2, $j_{ac}=50$ A/cm^2.

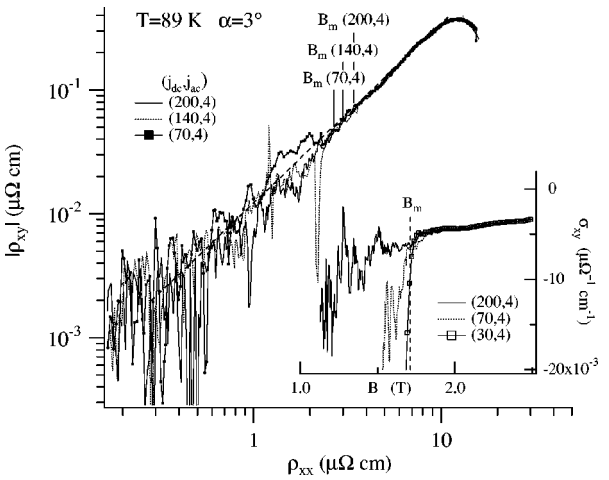

FIG. 6. Log-log plot of $|\rho_{xy}|$ vs ρ_{xx} for different current densities at 89 K and $\alpha=3°$. For each curve the current densities are indicated by (j_{dc},j_{ac}), both in units of A/cm^2. The position of the vortex-lattice melting field is indicated. The linear fit according to a scaling law $|\rho_{xy}|=A\rho_{xx}^{\beta}$ gives the average values $A\approx0.012$ and $\beta\approx1.4$ (see dashed line) and there is no current dependence of the parameters. Inset: The field dependence of the Hall conductivity σ_{xy} at 89 K, for various ac and dc current densities. The dotted vertical line denotes the vortex-lattice melting transition at B_m.

becomes negative below T_c. In the vortex-liquid phase the Hall conductivities at $\alpha=0°$ and $\alpha=7°$ coincide down to about T_{TB}. Below roughly T_{TB} and for $\alpha=0°$ we observe an approximately constant Hall conductivity until the large scattering of the data begins. For the angle tilted away from the c axis, $\alpha=7°$, the Hall conductivity decreases smoothly until the vortex-lattice melting transition occurs. Below T_m the Hall conductivity deviates from its behavior in the vortex-liquid phase and goes rapidly towards large negative values (see also the current dependence in Fig. 6 below). The Hall angle, not shown in Fig. 5, tends to small values.

We investigate now the Hall resistivity scaling behavior. The main panel of Fig. 5 shows the log-log plot of $|\rho_{xy}|$ vs ρ_{xx} for $\alpha=7°$ and $\alpha=0°$ at 2 T and large dc and ac current densities. The position of the vortex-lattice melting and Bose-glass temperatures are indicated. The fit to a power-law dependence of a form $|\rho_{xy}|=A\rho_{xx}^{\beta}$, gives for $\alpha=0°$ the values $A\approx0.005$ and $\beta\approx2.0$, and for $\alpha=7°$ it gives $A\approx0.02$ and $\beta\approx1.4$, as shown by the two straight dashed lines. A separate fit to the solid and liquid part gives the same result within the experimental error (we also obtain $\beta\approx1.4$ in the whole range 3° to 7°). *There is no change of the* $|\rho_{xy}|$ vs ρ_{xx} *dependence at the vortex-lattice melting transition or at the Bose-glass transition*, suggesting that such a scaling law is effectively insensitive to the specific vortex phase.

The Hall effect current dependence is shown in Fig. 6 for $\alpha=3°$. The inset of Fig. 6 shows the Hall conductivity σ_{xy} as a function of the magnetic field at 89 K and different dc currents. At $\alpha=3°$ the vortex phase transition is the vortex-lattice melting at B_m. The curves have larger noise over signal ratio than above. Nevertheless the current dependence is clearly observable in the diverging σ_{xy}. *Below the melting field* B_m *the Hall conductivity* σ_{xy} *decreases faster, the smaller the dc current.* Above B_m in the vortex-liquid the Hall conductivity is linear. The current dependence of the scaling law is investigated in the main panel of Fig. 6, which shows a log-log plot of $|\rho_{xy}|$ vs ρ_{xx}, constructed from measurements as a function of the magnetic field at a constant temperature of 89 K and different current densities. The fit to a power-law dependence of a form $|\rho_{xy}|=A\rho_{xx}^{\beta}$, with A and β free parameters as above, gives the average values $A\approx0.012$ and $\beta\approx1.4$. *There is no change of the scaling law with the current density*, neither in liquid nor in the Bragg-glass phases. Notice also that even if strictly speaking we measure the differential resistivity, which differs from the usual resistivity in the nonlinear voltage-current regime, the scaling law is unaffected by crossing from the linear (liquid) to the nonlinear (solid) vortex-phases.

As a conclusion of the experimental section, we underline that the general trend of the Hall resistivity is captured by a very robust scaling law $|\rho_{xy}|=A\rho_{xx}^{\beta}$. The scaling law implies $\tan\theta_H\propto\rho_{xx}^{\beta-1}$ and $\sigma_{xy}\propto\rho_{xx}^{\beta-2}$. Consistently, with an exponent less than two at $\alpha>\alpha^*$, as the longitudinal resistivity tends to zero, the Hall conductivity diverges, and the Hall angle is small. The strong nonlinear dependence of the longitudinal resistivity in the Bragg-glass phase is reflected in the Hall conductivity, which below the melting transition diverges faster, the smaller the current density. For $\alpha=0°$ and consistently with an exponent $\beta\approx2$ the Hall conductivity seems to be a constant below about T_{TB}, the temperature of twin-boundary pinning onset.

One could argue that in presence of high electric current densities, and at high magnetic fields such that the average distance between vortices is much less than the average separation between twins, the distinction of a moving Bragg-glass and a moving Bose-glass has not very much signification. However, our results show exactly the opposite: the scaling law, or the Hall conductivity, is different in the two

moving vortex phases, and the two vortex phases can be distinguished, at last with respect to the Hall behavior. Notice also that, since for $\alpha=0°$ the exponent $\beta\approx 2$ is observed below T_{TB}, not only the correlated twin disorder changes the nature of the static and dynamic vortex-solid phases (Bragg-glass to Bose-glass), but also induces two different vortex-liquids, with different dynamic properties.

III. DISCUSSION

A Hall resistivity that vanishes as a power of the longitudinal resistivity has been observed by various authors,[2,28,29] and predicted in different theoretical contexts (see Sec. I), but a complete explanation is not yet achieved. A consistent theory should explain the robustness of the scaling $\rho_{xy}\propto\rho_{xx}^{\beta}$ reported here. Our data suggest that a comprehensive theory for the Hall scaling law, far enough from the sign change, does not require phase-dependent parameters. Moreover, we have found that σ_{xy} becomes current dependent in the Bragg-glass phase. This contradicts the idea that the Hall conductivity is independent of pinning.[12]

A significant result of this paper is that the exponent β entering the scaling law is *disorder-type dependent*. In particular $\beta\approx 2.0$ for correlated planar disorder and $\beta\approx 1.4$ for uncorrelated pointlike disorder. This suggests an alternative explanation for the scaling behavior, as proposed by Geshkenbein.[30] If one views the vortex freezing as an inhomogeneous, nonsimultaneous process, with regions where vortices are pinned (thus with vanishing resistivity), and regions where they can still move (thus inducing a nonzero electric resistivity), the vortex freezing behavior in superconductors has strong analogies with the *percolation transition* in inhomogeneous conductors. In the case of a mixed metallic/insulating system, the conductivity is governed by percolation processes and the longitudinal conductivity is expressed as $\sigma_{xx}\propto\delta p^{t}$, where $\delta p=p-p_c$ is the difference between the conducting metallic phase density p and the critical percolation threshold density p_c. The critical exponent is $t\approx 1.3$ in two dimensions, and $t\approx 1.6$ in three dimensions.[31] Similarly, the Hall number R_H diverges as $R_H\propto\delta p^{-g}$, where $g=\nu(d-2)$,[31] where d is the dimension. In two dimensions $g=0$ and as a consequence the Hall conductivity $\sigma_{xy}\approx HR_H\sigma_{xx}^2$ is exactly proportional to σ_{xx}^2 (at constant magnetic field H). In three dimensions, $g=\nu\approx 0.9$,[31] such that $\sigma_{xy}\propto\sigma_{xx}^{2-g/t}\propto\sigma_{xx}^{1.44}$.

This immediately leads to a percolation model for the vortex scaling behavior, provided the vortex conductivity is interpreted as the electric resistivity of the metallic/insulating system, since a high vortex mobility means large electric dissipation, while high electronic mobility means low electric dissipation. With the identification that the conductivity σ in the metallic/insulating system is the resistivity ρ in the vortex system, one obtains the scaling law $\rho_{xy}\propto\rho_{xx}^{2-g/t}$ and $\beta=2-g/t$ for the vortex system. The percolation model is very appealing since it provides two universal exponents, i.e., $\beta=2$ and $\beta=1.44$, which correspond to the most frequently reported experimental estimate. These exponents are determined by the dimensionality of the vortex system, that is, determined by the vortex localization along correlated defects, or by the geometry of the samples. For the magnetic field accurately aligned to the twin boundaries, which localizes the vortices along the c axis, the system is two dimensional and $\beta\approx 2$. The same exponent is observed in two-dimensional films.[29] When the magnetic field is ''slightly'' tilted away from the twin boundaries (2°–3° are enough), the vortices recover the third degree of freedom and $\beta\approx 1.4$. This is also likely to happen when splayed defects are introduced by irradiation, bringing back the exponent form 2 to 1.5.[28]

ACKNOWLEDGMENTS

We are grateful to V. Geshkenbein and G. Blatter for many discussions. This work was supported by the Swiss National Science Foundation.

[1] A brief review of the experimental literature is given, for example, in S.J. Hagen, A.W. Smith, M. Rajeswari, J.L. Peng, Z.Y. Li, R.L. Greene, S.N. Mao, X.X. Xi, S. Bhattacharya, Qi Li, and C.J. Lobb, Phys. Rev. B **47**, 1064 (1993).

[2] J. Luo, T.P. Orlando, J.M. Graybeal, X.D. Wu, and R. Muenchausen, Phys. Rev. Lett. **68**, 690 (1992); A.V. Samoilov, *ibid.* **71**, 617 (1993).

[3] J.E. Hirsch and F. Marsiglio, Phys. Rev. B **43**, 424 (1991); R.A. Ferrell, Phys. Rev. Lett. **68**, 2524 (1992).

[4] M.V. Feigel'man, V.B. Geshkenbein, A.I. Larkin, and V.M. Vinokur, Pis'ma Zh. Éksp. Teor. Fiz. **62**, 840 (1995) [JETP Lett. **62**, 834 (1995)]; A. van Otterlo, M. Feigel'man, V.B. Geshkenbein, and G. Blatter, Phys. Rev. Lett. **75**, 3736 (1995).

[5] D.I. Khomskii and A. Freimuth, Phys. Rev. Lett. **75**, 1384 (1995).

[6] N.B. Kopnin and A.V. Lopatin, Phys. Rev. B **51**, 15 291 (1995).

[7] B. Wuyts, V. V. Moshchalkov, and Y. Bruynseraede, Phys. Rev. B **53**, 9418 (1996).

[8] Z.D. Wang and C.S. Ting, Phys. Rev. Lett. **67**, 3618 (1991); Z.D. Wang, J. Dong, and C.S. Ting, *ibid.* **72**, 3875 (1994).

[9] P. Ao, J. Supercond. **8**, 503 (1995); Chin. J. Phys. (Taipei) **36**, 190 (1998).

[10] H.J. Jensen, P. Minnhagen, E. Sonin, and H. Weber, Europhys. Lett. **20**, 463 (1992).

[11] A.T. Dorsey, Phys. Rev. B **46**, 8376 (1992); R.J. Troy and A.T. Dorsey, *ibid.* **47**, 2715 (1993).

[12] V.M. Vinokur, V.B. Geshkenbein, M.V. Feigel'man, and G. Blatter, Phys. Rev. Lett. **71**, 1242 (1993).

[13] A.T. Dorsey and M.P.A. Fisher, Phys. Rev. Lett. **68**, 694 (1992).

[14] R. Ikeda, J. Phys. Soc. Jpn. **65**, 3998 (1996).

[15] For a more complete bibliography see, for example, in E.H. Brandt, Rep. Prog. Phys. **58**, 1465 (1995).

[16] D.J. Thouless, Pin Ao, and Qian Niu, Phys. Rev. Lett. **76**, 3758 (1996); M.R. Geller, C. Wexler, and D.J. Thouless, Phys. Rev. B **57**, R8119 (1998); C. Wexler and D.J. Thouless, *ibid.* **58**, R8897 (1998).

[17] H.E. Hall and J.R. Hook, Phys. Rev. Lett. **80**, 4356 (1998); C. Wexler, D.J. Thouless, P. Ao, and Q. Niu, *ibid.* **80**, 4357 (1998); P. Ao, *ibid.* **80**, 5025 (1998); N.B. Kopnin and G.E. Volovik, *ibid.* **80**, 5026 (1998).

[18] T. Nagaoka, Y. Matsuda, H. Obara, A. Sawa, T. Terashima, I. Chong, M. Takano, and M. Suzuki, Phys. Rev. Lett. **80**, 3594 (1998).

[19] G. D'Anna, V. Berseth, L. Forró, A. Erb, and E. Walker, Phys. Rev. Lett. **81**, 2530 (1998).
[20] P. Ao, Phys. Rev. Lett. **82**, 2413 (1999); R. Ikeda, *ibid.* **82**, 3378 (1999).
[21] V. Berseth, Ph.D. thesis, Ecole Polytechnique Fédérale de Lausanne, 1999.
[22] H. Safar, P.L. Gammel, D.A. Huse, D.J. Bishop, J.P. Rice, and D.M. Ginsberg, Phys. Rev. Lett. **69**, 824 (1992); W.K. Kwok, S. Fleshler, U. Welp, V.M. Vinokur, J. Downey, G.W. Crabtree, and M.M. Miller, *ibid.* **69**, 3370 (1992).
[23] S.A. Grigera, E. Morré, E. Osquiguil, C. Balseiro, G. Nieva, and F. de la Cruz, Phys. Rev. Lett. **81**, 2348 (1998).
[24] D.R. Nelson and V.M. Vinokur, Phys. Rev. Lett. **68**, 2398 (1992); Phys. Rev. B **48**, 13 060 (1993).
[25] See, for example, P. Le Doussal and T. Giamarchi, Phys. Rev. B **57**, 11 356 (1998).
[26] G. Blatter, M.V. Feigel'man, V.B. Geshkenbein, A.I. Larkin, and V.M. Vinokur, Rev. Mod. Phys. **66**, 1125 (1994).
[27] M. Roulin, A. Junod, A. Erb, and E. Walker, Phys. Rev. Lett. **80**, 1722 (1998).
[28] R.C. Budhani, S.H. Liou, and Z.X. Cai, Phys. Rev. Lett. **71**, 621 (1993); A.V. Samoilov, A. Legris, F. Rullier-Albenque, P. Lejay, S. Bouffard, Z.G. Ivanov, and L.-G. Johansson, *ibid.* **74**, 2351 (1995); W.N. Kang, D.H. Kim, S.Y. Shim, J.H. Park, T.S. Hahn, S.S. Choi, W.C. Lee, J.D. Hettinger, K.E. Gray, and B. Glagola, *ibid.* **76**, 2993 (1996).
[29] P.J.M. Wöltgens, C. Dekker, and H.W. de Wijn, Phys. Rev. Lett. **71**, 3858 (1993).
[30] V. Geshkenbein (private communication).
[31] B.I. Shklovskii, Zh. Éksp. Teor. Fiz. **72**, 288 (1977) [Sov. Phys. JETP **45**, 152 (1977)]; J.P. Straley, J. Phys. C **13**, 4335 (1980).